Sorption of Cm(III) and Gd(III) onto gibbsite, α-Al(OH)$_3$: A batch and TRLFS study

N. Huittinen [a,*], Th. Rabung [b], J. Lützenkirchen [b], S.C. Mitchell [c], B.R. Bickmore [d], J. Lehto [a], H. Geckeis [b]

[a] *Laboratory of Radiochemistry, University of Helsinki, P.O. Box 55, FIN-00014 University of Helsinki, Finland*
[b] *Institut für Nukleare Entsorgung, Forschungszentrum Karlsruhe, P.O. Box 3640, D-76021 Karlsruhe, Germany*
[c] *Anadarko Petroleum Corporation, 1201 Lake Robbins Dr., The Woodlands, TX 77380, USA*
[d] *Department of Geological Sciences, Brigham Young University, Provo, UT 84602, USA*

ABSTRACT

Gd(III) and Cm(III) sorption onto a pure aluminum hydroxide, gibbsite (α-Al(OH)$_3$), is studied by batch experiments and time-resolved laser fluorescence spectroscopy (TRLFS). The experiments are conducted under argon atmosphere to exclude the influence of atmospheric CO_2 on solution and surface speciation. Batch experiments are done in two different electrolytes 0.1 M NaClO$_4$ and 0.1/0.01 M NaCl at a constant gibbsite concentration of 2.2 g/L. Gadolinium concentrations are varied from 6.4×10^{-9} to 6.4×10^{-5} M. pH-dependent sorption is found to be congruent at Gd(III) concentrations up to 6.4×10^{-7} M and a shift of the pH edge to higher pH values is observed for higher metal ion concentrations. Type of background electrolyte anion and ionic strength do not affect the metal ion sorption. The spectroscopic investigations are performed with Cm(III) and gibbsite concentrations of 2×10^{-7} M and 0.5 g/L, respectively. From the strongly red-shifted emission spectra two different inner-sphere surface complexes can be identified. A third species appearing at pH 6–11 is assigned to a coprecipitated or incorporated Cm(III) species. This incorporated species is most likely formed as a consequence of the applied experimental procedure. By continuously increasing the pH from 4 we move from high to low gibbsite solubility domains. As a result, aluminum hydroxide precipitates from oversaturated solutions, either covering already adsorbed curium or forming a Al/Cm(OH)$_3$ coprecipitate. Fluorescence lifetimes for the surface-bound Cm(III) complexes and the incorporated species are at 140–150 and 180–200 μs, respectively. Emission bands of the Cm(III) gibbsite surface complexes appear at comparable wavelengths as reported for Cm(III) species bound to aluminum oxides, e.g., γ-Al$_2$O$_3$; however, lifetimes are longer. This could presumably arise from either shorter binding distances of the Cm to Al–O sites or a coordination to more surface sites.

© 2008 Elsevier Inc. All rights reserved.

1. Introduction

Deep geological clay and bedrock formations are considered appropriate for the final disposal of nuclear waste. Scenarios assuming accidental groundwater inflow to the repository must take into account the release of radionuclides into the geosphere. Radionuclide retention or retardation can take place via various solid–solute interaction mechanisms. For nuclear safety assessment it is therefore imperative to understand the chemistry behind radionuclide reactions at the groundwater–mineral interface, including characterization of the surface species and determination of involved mechanisms. The long-term radiotoxicity of nuclear waste is dominated mainly by the transuranium elements. The prevailing geochemical conditions in the repository dictate their speciation and thus their mobility. Under the reducing conditions of deep geological formations, actinides are usually found in their reduced oxidation states III and/or IV.

Extensive studies of metal ion sorption on different aluminum oxides/hydroxides have been performed [1–5]. Pure aluminum oxides/hydroxides are rare in nature, but these minerals contain reactive aluminol groups also present at the surfaces of aluminosilicates which are abundant in natural systems. Furthermore, aluminum oxides/hydroxides display similar mineralogical structures as iron oxides/hydroxides and can thus be used as models for these iron-containing minerals, which are not transparent for visible light and therefore not suitable for investigation by a variety of spectroscopic studies such as Time-Resolved Laser Fluorescence Spectroscopy (TRLFS). The reactivity of aluminol groups differs with varying atomic arrangements on the mineral surface, leading to slightly different metal ion sorption behavior on different aluminum oxides/hydroxides. In aqueous solutions the surfaces of suspended oxides are hydrated, and surface transformations of oxides like α-Al$_2$O$_3$ and γ-Al$_2$O$_3$ have been reported [6–8]. Investigations on γ-alumina show a surface transformation into bayerite,

β-Al(OH)$_3$ [6,7], a secondary phase formation that presumably changes the reactivity of the mineral surface. A similar secondary phase formation has been reported for α-alumina, where a surface transformation into bayerite or gibbsite, α-Al(OH)$_3$, has been observed [8,9]. The aim of this work is to study trivalent metal ion sorption onto a pure aluminum hydroxide. For this purpose the mineral gibbsite was chosen. As noted before, gibbsite forms at the α-alumina/water interface and is thermodynamically more stable in aqueous solution than the corresponding aluminum oxides. Results from previous work by Rabung et al. [10,11] and Stumpf et al. [12], where the sorption of trivalent actinides onto both α- and γ-alumina has been investigated, are compared with the findings of the present study. Curium is a minor actinide element in the nuclear waste, but exhibits excellent fluorescent properties suitable for surface speciation investigation by means of TRLFS. It was therefore chosen in our experiments to represent trivalent actinides such as americium, which is far more abundant. Batch sorption studies were carried out with the trivalent lanthanide ion gadolinium, which is usually considered as a chemical homologue to curium and americium.

2. Materials and methods

2.1. Gibbsite—synthesis and characterization

The gibbsite used throughout this work was prepared through precipitation of Al(OH)$_3$ followed by subsequent dialysis of the suspension at 70 °C for a time span of 4 months. A 0.33 M aluminum chloride solution was titrated with 1 M NaOH until a pH value of 4.5, at which amorphous aluminum hydroxide precipitates. The precipitation was carried out in a glove box under argon atmosphere (O$_2$ <1 ppm) to eliminate possible contamination by atmospheric CO$_2$. The aluminum hydroxide precipitate was dialyzed against deionized water (MilliQ) at a temperature of 70 °C. Water exchange was done every day for the first four weeks, and 2–3 times per week for another 3 months. The pH and solid content of the final suspension were 4.2 and 41.9 ± 1 g/L, respectively. Gibbsite particles are shaped as hexagonal platelets, with predominant basal plane contribution to overall surface area, and comparatively small edge planes, Figs. 1a and 1b. The diameter and height of these particles were determined with atomic force microscopy, AFM, and N$_2$-BET analysis was done to evaluate the specific surface area of the mineral. Mineralogical purity and surface composition were examined with XRD (Bruker D8Advance) and X-ray photoelectron spectroscopy, XPS, respectively. To determine the isoelectric point, IEP of the mineral, i.e., the pH value at which the net surface charge equals zero, ζ-potential measurements (Zeta Plus, Zeta Potential Analyser, Brookhaven Instruments Corporation) were performed in 0.1/0.01 M NaClO$_4$ and MilliQ water. The gibbsite suspension was diluted in the three different media to a final concentration of 1 g/L. pH adjustments were done from 4.95 to approximately 12 with NaOH.

For studies requiring solid gibbsite samples or freshly resuspended gibbsite, a fraction of the synthesized gibbsite batch was freeze-dried.

2.2. Batch sorption experiments

Batch sorption experiments were conducted in a glove box under argon atmosphere (O$_2$ <1 ppm) to exclude atmospheric CO$_2$ which influences the solution speciation of trivalent actinides through the formation of carbonate species at pH values above 6 [13] that may adsorb onto gibbsite. All reagents were prepared in the glove box and MilliQ water was stored in an open bottle inside the glove box to minimize the CO$_2$ content prior to use. Gadolinium sorption onto gibbsite was investigated as a function of pH in different electrolytes and ionic strengths (0.1 M NaClO$_4$ and 0.1/0.01 M NaCl). The gibbsite concentration was fixed to 2.2 g/L in each batch, while the Gd^{3+} concentration was varied between 6.4×10^{-9} and 6.4×10^{-5} M. pH adjustments were done in small steps by addition of CO$_2$-free NaOH. The sample solutions were shaken periodically for 3–7 days to reach sorption equilibrium. After the equilibration time the samples were centrifuged at 18,000 rpm and the aluminum and gadolinium concentrations were analyzed in the supernatant by ICP-MS.

2.3. TRLFS study

Samples for TRLFS measurements were prepared under the same conditions as the batch experiments. Two series of three parallel samples were prepared in 0.1 M NaClO$_4$ with gibbsite and curium concentrations of 0.5 g/L and 2×10^{-7} M, respectively. For one series the stock gibbsite suspension was diluted directly in the electrolyte. Those experiments are referred to in the following text as "gibbsite suspension." The other series was prepared by using freeze-dried gibbsite resuspended in the electrolyte (referred to as "freeze-dried gibbsite I"). For comparison experiments were performed with another freeze-dried gibbsite (referred to as "freeze-dried gibbsite II") previously characterized by Mitchell [14]. Suspensions were shaken periodically for 2–3 days to reach sorption equilibrium. The TRLFS measurements were performed with a pulsed Nd:YAG pumped dye laser system (Continuum, Powerlite, ND 6000, laser dye; Exalite 398). The Cm(III) fluorescence emission was detected using an optical multichannel analyzer consisting of a polychromator (Chromex 250) with a 1200 lines/mm grating. The emission spectra were recorded in the range 580–620 nm, 1 µs after the exciting laser pulse in a time window of 1 ms. The excitation wavelength used was 396.6 nm. For the lifetime measurements the time delay between the laser pulse and the camera gating was scanned between 1 and 1200 µs in intervals of 10–15 µs. The laser pulse energy, controlled by a photodiode, was between 2.5 and 3.5 mJ during all measurements.

3. Results

3.1. Gibbsite—synthesis and characterization

The XRD study showed the mineralogical purity and crystalline character of the synthetic bulk gibbsite. The analysis of the gibbsite surface composition with XPS revealed the presence of small amounts of chloride (0.16% of total atomic concentration) originating from the use of AlCl$_3$ for synthesis. As the gibbsite surface is positively charged under stock suspension conditions (pH 4.2) the presence of the respective amounts of Cl$^-$ is expected. The aluminum to oxygen ratio was analyzed from the peak intensities in the XPS spectrum, and was determined to be 0.329, in very good agreement with the theoretical value of 0.333. The gibbsite particle diameter and height assessed from 25 particles in the AFM survey were 250 ± 60 and 16.8 ± 10.4 nm, respectively. The specific surface area of the platelets was determined to be 49.5 m^2/g. The pH value 11.0 was obtained for the IEP of gibbsite. Respective pH-dependent ζ-potential data are shown in Fig. 2.

3.2. Gadolinium sorption onto gibbsite

Figs. 3 and 4 present data for pH-dependent fraction of sorbed Gd (%) and log K_d vs pH, respectively, for Gd concentrations ranging from 6.4×10^{-9} to 6.4×10^{-5} M in 0.1 M NaClO$_4$. pH curves are congruent at Gd concentrations up to 6.4×10^{-7} M. Uptake starts above pH 5.5 and is complete at around pH 7.5. At metal ion concentrations of 6.4×10^{-6} and 6.4×10^{-5} M a shift of the pH curve to higher pH values occurs and complete sorption is attained at
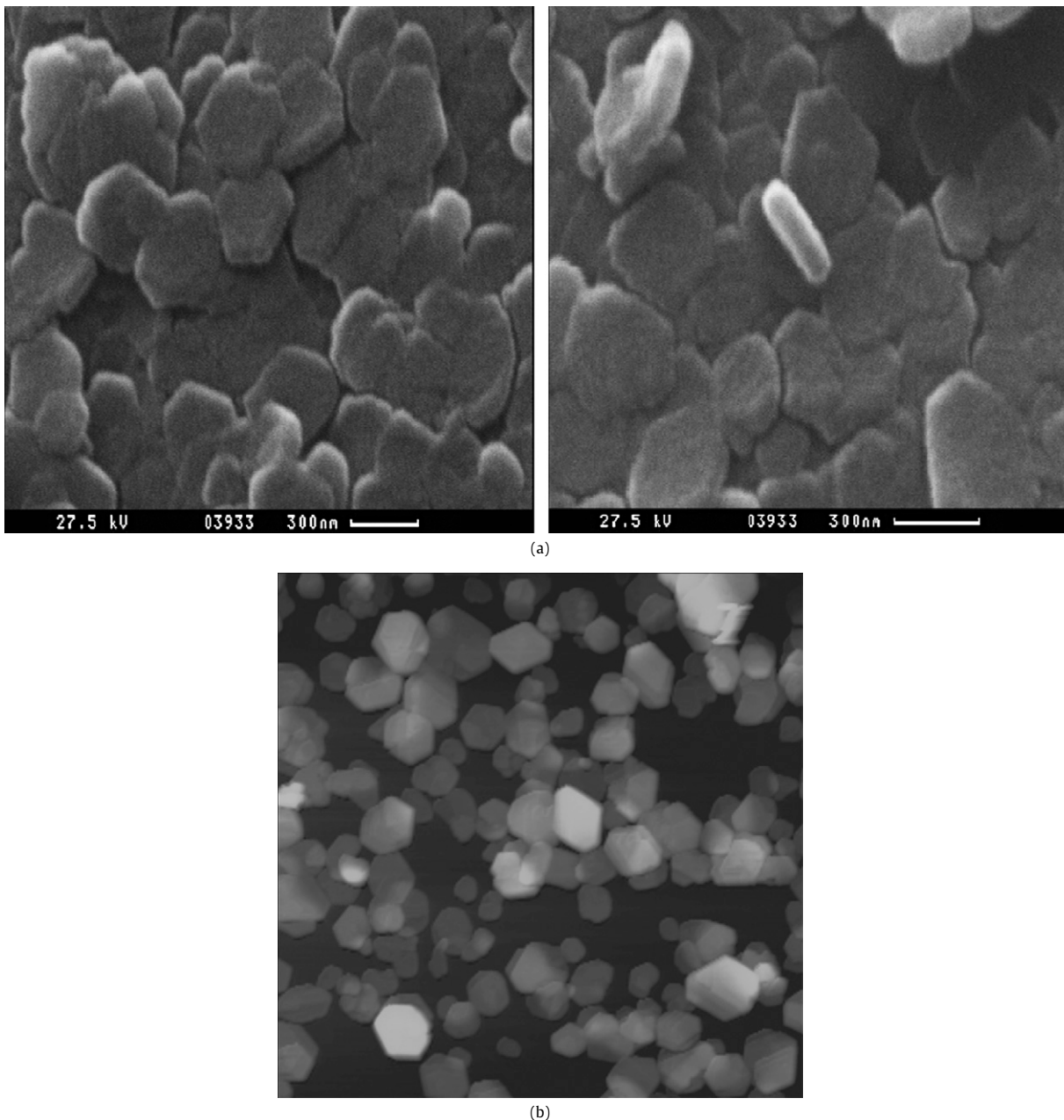
Fig. 1. (a) SEM images and (b) AFM image of the synthesized gibbsite.

pH 8.5 instead of 7.5. In the ideal sorption range (linear isotherm) the position of the pH edge at a given solid concentration is independent of the metal ion concentration as observed in the present study for Gd concentrations up to 6.4×10^{-7} M. At higher metal ion concentrations deviations from ideal sorption behavior cause a shift of the pH edge to higher pH values. Nonideal behavior may result, for example, from saturation effects or surface binding site heterogeneity [15]. At the highest Gd concentration used in the present study, a saturation of 35% of the singly coordinated surface hydroxyl sites on the gibbsite edge planes was calculated, using an average value of 8.5 nm^{-2} (data taken from [16,17]) for the surface site density and assuming sorption taking place as monodentate surface complex formation only at crystal edges. Surface sites would be completely saturated by sorbed metal ions if we suppose tridentate binding of trivalent Gd. However, binding to both edge and basal plane surface sites with different stoichiometries cannot be excluded. In addition to the sorption studies where Gd concentrations were varied, the effect of both the electrolyte anion ClO_4^-/Cl^- and different ionic strength 0.1/0.01 M NaCl was examined. The perchlorate anion has not been found to influence metal ion sorption onto various minerals; however, some effects on, e.g., Cm(III) complexation have been observed for the chloride anion at high Cl$^-$ concentrations [18]. For the range of ionic strengths used in the present study no such influence was detected and thus experimental data of performed investigations are not included.

3.3. Curium sorption onto gibbsite

3.3.1. Curium emission spectra

Figs. 5 and 6 present the curium emission spectra for experiments with the two gibbsite samples, gibbsite suspension and freeze-dried gibbsite I, normalized to the highest peak intensities. The latter series resulted in emission spectra with quite low fluorescence emission intensities. Most likely, this is due to larger gibbsite particles as a result of the previous drying treatment, re-
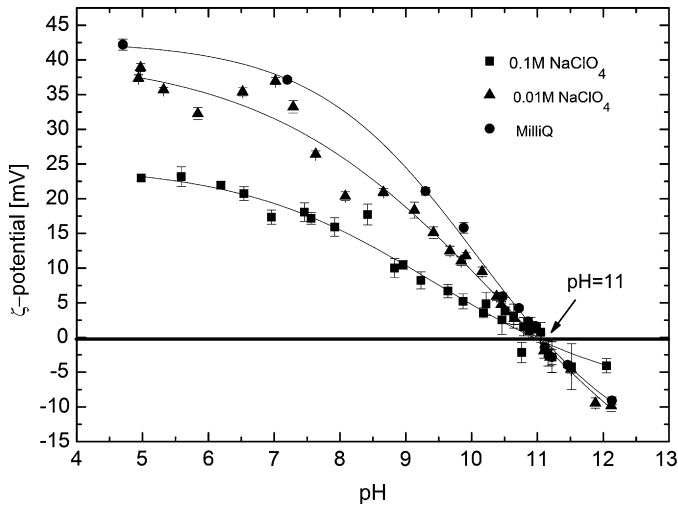
Fig. 2. Zeta potential diagram. The gibbsite concentration in all three media, 0.1 M NaClO$_4$, 0.01 M NaClO$_4$, and MilliQ water, was 1 g/L.
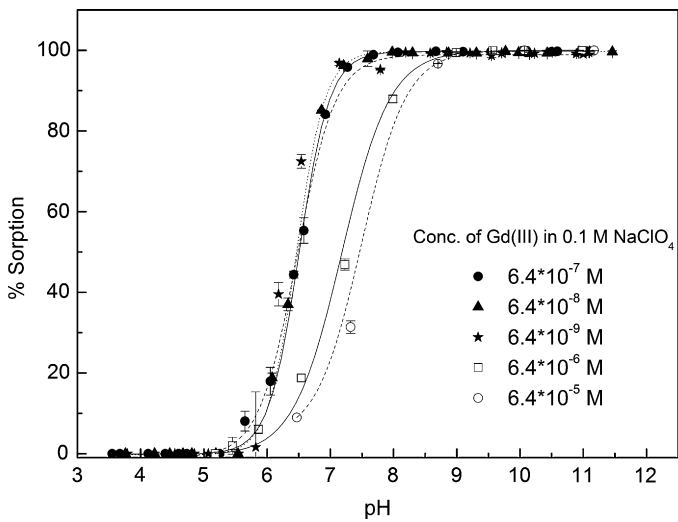
Fig. 3. pH-dependent Gd sorption onto gibbsite. Gd concentrations: 6.4×10^{-9}–6.4×10^{-5} M in 0.1 M NaClO$_4$, 2.2 g/L gibbsite.
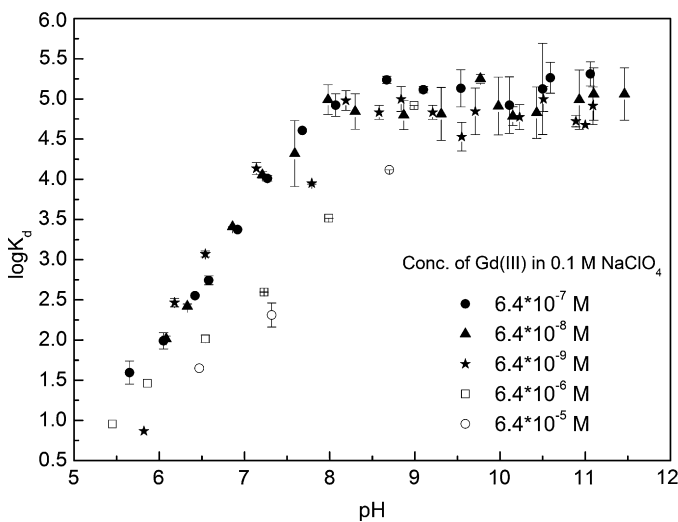
Fig. 4. Gd sorption to gibbsite plotted as $\log K_d$ vs pH; Gd concentrations: 6.4×10^{-9}–6.4×10^{-5} M in 0.1 M NaClO$_4$, 2.2 g/L gibbsite.
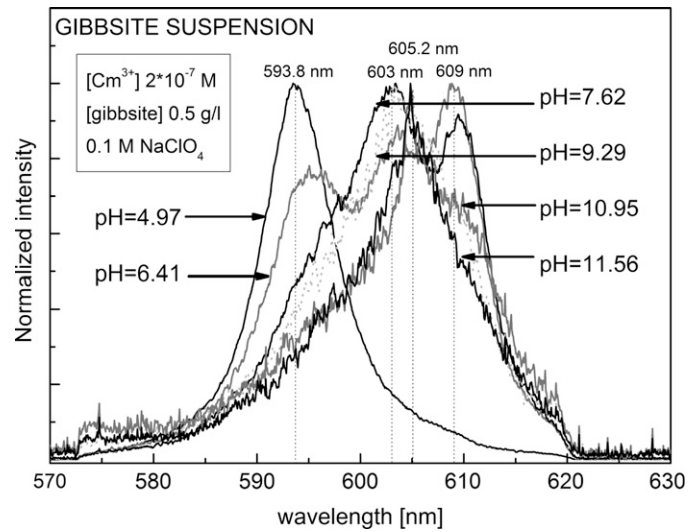
Fig. 5. Curium emission spectra of the sample series "gibbsite suspension."
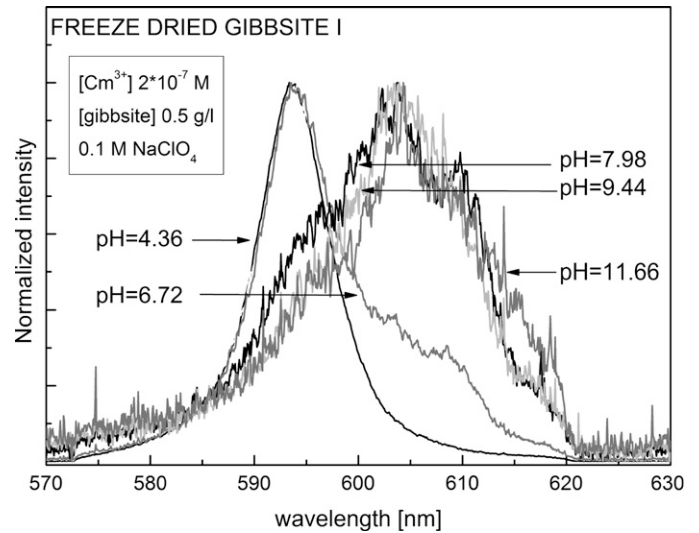
Fig. 6. Curium emission spectra of the sample series "freeze-dried gibbsite I."

sulting in intensity losses due to laser light scattering. As observed in previous investigations on curium sorption onto various aluminum oxides [11,12], our curium emission spectra show only one emission peak with a maximum at 593.8 nm for pH values below 5. This peak is assigned to the curium aquo ion. The curium aquo ion peak disappears as the pH is raised and sorption onto the mineral surface increases. As a consequence emission bands are red-shifted and the development of peak maxima at about 603.0 and 605.2 nm is observed. A surprising difference in emission spectra obtained in this study, when compared to previous investigations, is the appearance of a resolved peak at about 609 nm. This peak develops in the pH range from 6 to 11. The contribution of this species increases up to pH 9, decreases when pH is further raised to 11, and disappears at higher pH. This emission band is much less discernible in respective experiments with freeze-dried gibbsite I (Fig. 6). In order to verify those results, we performed additional experiments with a different gibbsite batch synthesized in a different laboratory (freeze-dried gibbsite II). Respective pH-dependent spectra for Cm sorbed to gibbsite are shown in Fig. 7. Similar to the spectra obtained with our freeze-dried gibbsite I the Cm emission band at $\lambda = 609$ nm becomes only visible as a shoulder in the pH range 8.8–9.5. Various cross-check experiments were
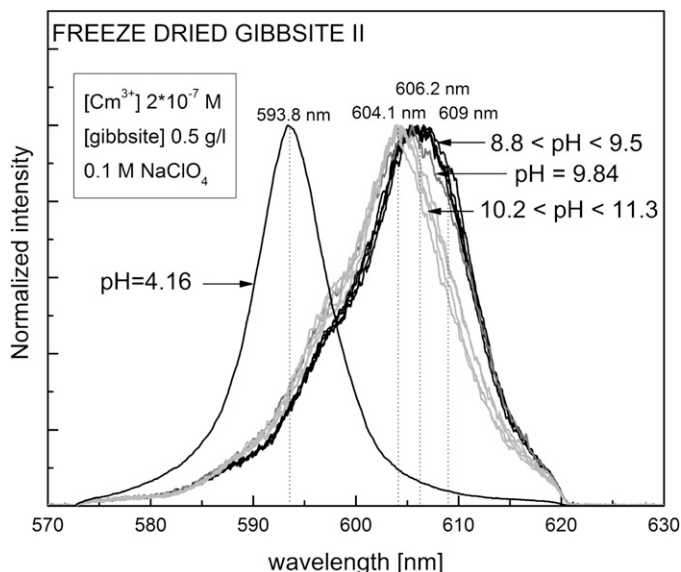
Fig. 7. Curium emission spectra of the sample series "freeze-dried gibbsite II."

Fig. 8. The fitted fluorescence decay curves for the sample series "gibbsite suspension."

performed in order to rule out possible contaminations of sorbent or solutions as a reason for the spectroscopic findings.

3.3.2. Fluorescence lifetimes

Fluorescence lifetimes of actinides in aquatic environment are relatively short, due to the energy transfer from excited f levels to lower lying vibronic states of water molecules in first coordination sphere of the actinide. When the actinide cation is adsorbed onto a mineral surface by inner-sphere complexation, some of the H_2O molecules in the first coordination sphere are displaced, resulting in extended fluorescence lifetimes. For Cm a correlation between the number of water molecules in the hydration sphere and the fluorescence decay constant k_{obs} has been stated [19]:

$$nH_2O = 0.65 \times k_{obs}(Cm) - 0.88. \tag{1}$$

Here $k_{obs} = 1/\tau$, where τ is the fluorescence lifetime in milliseconds.

Fluorescence lifetimes were recorded for both experiment series with the gibbsite suspension and the freeze-dried gibbsite I. In all cases at least biexponential decay curves were observed and prohibited an unambiguous deconvolution of separate lifetimes for individual species. For the aquo ion the lifetime observed was 68 μs, a value typically found in the literature [20]. For the gibbsite-sorbed species at least two lifetime components with 140–150 and 180–200 μs could be extracted. The fitted lifetime curves for the gibbsite suspension series are presented in Fig. 8. The aquo ion with $\tau = 68$ μs is known to correspond to a species surrounded by 9 water molecules in solution. Lifetimes in the range of 140–150 μs point to the presence of on average 3.5–3.8 H_2O/OH^- entities left in the first hydration sphere, 180–200 μs corresponds to 2.4–2.7 H_2O/OH^- according to Eq. (1). By correlation of measured lifetimes with the pH dependence of the appearance of the emission bands, the shorter lifetime component can be attributed to species with emission bands at $\lambda_{max} = 603.0$ and 605.2 nm while the longer lifetime is associated with the peak at $\lambda_{max} = 609$ nm.

4. Discussion

Three peak maxima at 600.6, 602.5, and 605.7 nm have been identified by Rabung et al. [11] after peak deconvolution in their investigation of Cm sorption onto γ-alumina. The spectra were assigned to the curium inner-sphere surface complexes
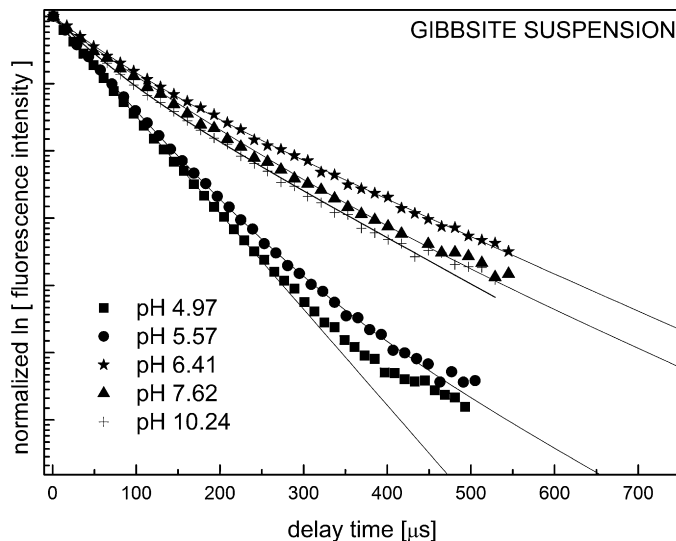
$[>Al–O–An(III)(H_2O)_5]^{2+}$, $[>Al–O–An(III)(OH)(H_2O)_4]^+$, and $[>Al–O–An(III)(OH)_2(H_2O)_3]$ appearing successively with increasing pH. Peak positions found in the present study are similar (603.0 and 605.2 nm). The species with $\lambda_{max} = 609$ nm with unexpected pH-dependent behavior will be discussed separately. The Cm species characterized by a peak maximum at 600.6 nm as found in experiments with γ-alumina at around pH 6, however, was not observed. This might be explained by the relatively high isoelectric point of our gibbsite (pH_{iep} 11.0) which indicates the predominance of protonated surface functional groups (formation of $>Al–OH_2^+$) over a wide pH range, inducing a positive surface charge. Consequently, Cm/Gd sorption to gibbsite starts at higher pH compared to γ-alumina with a lower pH_{iep} ($\sim$9). Sorption to γ-alumina starts at pH $>$4.5 under comparable experimental conditions [21]. One could, therefore, assume that the first Cm surface species being dominant at the γ-alumina surface in a narrow range around pH 6 does not significantly contribute to the Cm surface speciation at gibbsite, where sorption starts at only slightly lower pH. However, fluorescence lifetimes measured for Cm on gibbsite are clearly higher than those found for Cm–γ-alumina ($\sim$110 μs), corresponding to 5 H_2O/OH^- left in the first Cm coordination sphere.

Cm species sorbed onto sapphire (012), (110), (018), and (104) single crystal surface planes show, different from those sorbed onto γ-alumina, a relatively strong red-shifted fluorescence emission band ($\lambda_{max} = 603.6$ nm) at even lower pH and lifetimes of 158–192 μs comparable to what we find for Cm–gibbsite. Based also on XPS results, the more red-shifted spectra obtained in the sapphire study were interpreted to arise from Cm bound either closer to the Al_2O_3 surface and/or a coordination to more $>Al–OH$ groups than at the γ-alumina surface. This explains the longer fluorescence lifetimes corresponding to 2.5–3.2 H_2O/OH^- in the first Cm coordination sphere. Fluorescence lifetimes (140–150 μs) and the peak position of the first Cm–gibbsite species are comparable to those of sapphire-bound species, suggesting comparable chemical environments. The second gibbsite surface-sorbed species ($\lambda_{max} = 605.2$ nm) appearing at higher pH can then be interpreted as a hydrolyzed Cm surface species, analogously to the assignment of γ-alumina sorbed Cm in the same pH region.

Published emission band maxima for surface-bound Cm are usually found at $\lambda_{max} \leqslant 607$ nm [22]. The strong red-shift in spectra up to 609 nm, the longer lifetimes, and the nonexpected pH-dependent appearance of this band are distinct indications for the appearance of a Cm species different from a surface complex.
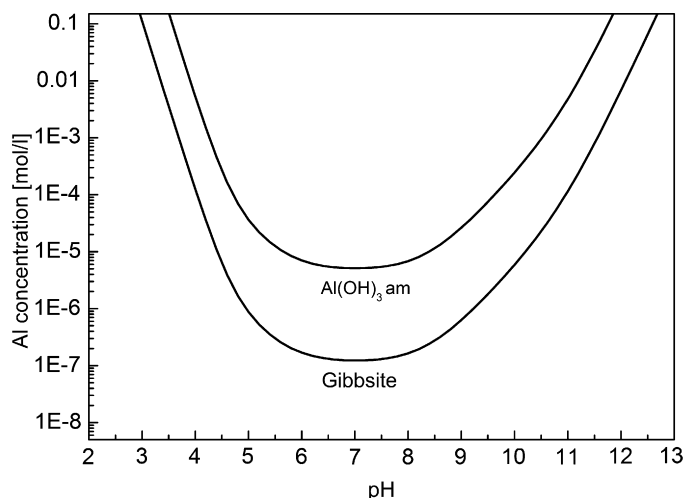
Fig. 9. Solubility curve for gibbsite and amorphous Al(OH)$_3$.

Fig. 10. Curium emission spectra of the "freeze-dried gibbsite II" sample after addition of 10^{-4} M aluminum.

TRLFS suggests the existence of a strong ligand field effect pointing to the occurrence of a coprecipitation or incorporation mechanism. Our experiments were conducted by successively increasing the pH in the gibbsite suspension after Cm addition starting from pH ∼4. According to the known solubility curve for gibbsite (see Fig. 9; data for calculations taken from [23]) Al solubility decreases with increasing pH, passes a minimum at pH ∼7, and increases again with increasing pH due to the formation of anionic aluminate species. Consequently, our experiments generate oversaturation conditions for dissolved Al species with respect to solid Al(OH)$_3$ phases in the pH range ∼5 to ∼10. The fact that the Cm species with $\lambda_{max} = 609$ nm appears in a pH region ranging from 6 to 9 and then decreases again suggests coprecipitation of Cm with newly forming Al(OH)$_3$ or coverage of already adsorbed Cm by Al(OH)$_3$ growing at the gibbsite surface. When Al solubility increases at alkaline pH, newly formed Al(OH)$_3$ redissolves and only surface complexed Cm can be detected.

To support the hypothesis, freeze-dried gibbsite II sample contacted with curium was allowed to age for 15 days at pH 6.8. After this period of time, the sample was measured again. No peak at 609 nm could be observed in the emission spectrum. Al ions at a concentration of 10^{-4} M were added to the suspension to exceed the solubility limit of aluminum hydroxide, and the emission spectrum was recorded 0–4 days after Al addition. One day after the addition, a peak close to 609 nm developed and even increased with time up to 4 days (see Fig. 10). This finding supports the hypothesis of Cm interaction with Al related to oversaturation of gibbsite and thus potential incorporation at the aluminum hydroxide surface and explains the unexpected spectral evolution with pH.

The fact that the emission peak of incorporated Cm was less resolved in the sample series with freeze-dried gibbsite I and freeze-dried gibbsite II compared to experiments with the gibbsite suspension can be explained by the slow dissolution of freeze-dried gibbsite samples. Obviously, freeze-dried gibbsite does not equilibrate with the aqueous solution within the few days after preparation of the suspension and spectroscopic experiment. Due to the lower concentration of dissolved Al in those suspensions Cm incorporation is less relevant.

Fluorescence lifetimes measured for the incorporated species are comparatively short. Complete loss of the hydration sphere is reported for Cm included in various mineral structures with lifetimes exceeding 500 μs [22]. However, Cm coprecipitation with another solid hydroxide, brucite, Mg(OH)$_2$, resulted in a shift of the Cm fluorescence emission to 610.8 nm and a lifetime of only 165 μs [24], similar to our observations. Lifetimes at 180–200 μs
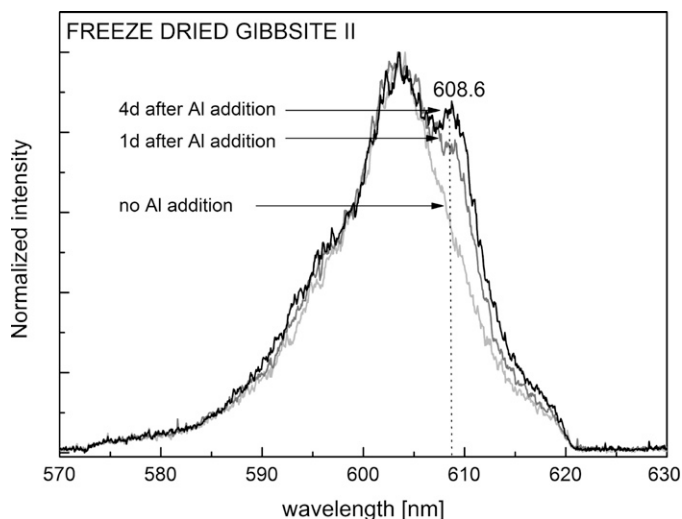
may be interpreted by insertion of Cm species into the gibbsite or coprecipitated structure keeping 2.4–2.7 H$_2$O/OH$^-$ entities in its primary hydration sphere. However, it is not entirely clear how and to which extent hydroxide ions in the crystal structure contribute to fluorescence quenching. Energy transfer from the excited Cm state to OH vibrational levels in the solid is controlled by various parameters [22]. In order to quantify the quench contribution of OH$^-$ ions in the Al(OH)$_3$, the Cm location and coordination within the solid and corresponding Cm–OH distances are required.

5. Conclusions

The results of the present study reveal two modes of Cm interaction with gibbsite: inner-sphere surface complexation and incorporation into the solid matrix. TRLFS parameters (peak position, lifetimes) obtained for the inner-sphere surface complexes are comparable to what has obtained for Cm sorbed to various sapphire surface planes ((012), (110), (018), and (104)). Lifetimes in general are longer than those obtained for Cm sorbed to sapphire (001) and γ-alumina. For the latter species a combined TRLFS and EXAFS study has been performed and a tentative structure for the Cm surface species was suggested: Cm is located in a distance of 2.45 Å to 4 oxygen atoms of the γ-alumina surface and is coordinated by 5 water molecules. A similar structure has been suggested for Cm sorbed on montmorillonite [25] and Y on rutile [26]. The longer lifetime obtained for the Cm–gibbsite species indicates less coordination with H$_2$O molecules which could be due to a closer Cm distance to the gibbsite surface or a higher coordination to gibbsite surface oxygen atoms. In both cases, coordination to 5 water molecules is sterically hindered, and explains the experimentally observed decrease of the hydration number. EXAFS experiments are planned to provide structural information.

The identification of an incorporated Cm species as a consequence of pH variations in our experiment might be considered as an experimental artifact in a first instance. It is, however, a clear proof that mineral surfaces cannot be considered as "inert" with regard to chemical variations as done in many studies. An incorporation process as described here would not have been detected by simple batch sorption experiments. In forthcoming experiments we will prepare a gibbsite batch stored at around pH 7, i.e., at the solubility minimum of gibbsite. Sorption measurements will then be performed starting from the gibbsite solubility minimum by varying the pH to the acidic range and to the alkaline range. By this procedure, precipitation of Al(OH)$_3$ solid should be avoided

and thus also Cm incorporation. We would nevertheless emphasize that actinide incorporation into minerals with dynamic surfaces is quite well known (e.g., calcite) and may also happen when the solid is in equilibrium with the aqueous phase [27].

Surface complexation modeling has been planned to support experimental work and to complete the study on Cm(III) and Gd(III) sorption onto gibbsite.

Acknowledgments

References

[1] O. Tochiyama, H. Yamazaki, N. Li, J. Nucl. Sci. Technol. 33 (1996) 846–851.
[2] Sh. Yu, X. Li, A. Ren, D. Shao, Ch. Chen, X. Wang, J. Radioanal. Nucl. Chem. 268 (2006) 387–392.
[3] H.X. Zhang, Z. Dong, Z.Y. Tao, Colloids Surf. A 278 (2006) 46–52.
[4] D. Xu, Q.L. Ning, X. Zhou, C.L. Chen, X.L. Tan, A.D. Wu, X. Wang, J. Radioanal. Nucl. Chem. 266 (2005) 419–424.
[5] N. Baumann, V. Brendler, T. Arnold, G. Geipel, G. Bernhard, J. Colloid Interface Sci. 290 (2005) 318–324.
[6] G. Lefevre, M. Duc, P. Lepeut, R. Caplain, M. Fedoroff, Langmuir 18 (2002) 7530–7537.
[7] C. Dyer, P.J. Hendra, W. Forsling, M. Ranheimer, Spectrochim. Acta Part A 49 (1993) 691–705.
[8] S. Desset, O. Spalla, P. Lixon, B. Cabane, Colloids Surf. A 196 (2002) 1–10.
[9] P.J. Eng, T.P. Trainor, G.E. Brown, G.A. Waychunas, M. Newville, S.R. Sutton, M.L. Rivers, Science 288 (2000) 1029–1033.
[10] Th. Rabung, D. Schild, H. Geckeis, R. Klenze, Th. Fanghanel, J. Phys. Chem. B 108 (2004) 17160–17165.
[11] Th. Rabung, H. Geckeis, X.K. Wang, J. Rothe, M.A. Denecke, R. Klenze, Th. Fanghänel, Radiochim. Acta 94 (2006) 609–618.
[12] T. Stumpf, Th. Rabung, R. Klenze, H. Geckeis, J.I. Kim, J. Colloid Interface Sci. 238 (2001) 219–224.
[13] V. Neck, T Fanghänel, J.I. Kim, Wissenschaft. Ber. FZKA-6110 (1998).
[14] S.C. Mitchell, An Improved MUSIC Model for Gibbsite, Brigham Young University, USA, 2005.
[15] P.W. Schindler, W. Stumm, Aquatic Surface Chemistry, Wiley–Interscience, New York, 1987, pp. 83–107.
[16] T. Hiemstra, H. Young, W.H. van Riemsdijk, Langmuir 15 (1999) 5942–5955.
[17] J. Rosenqvist, Surface Chemistry of Al and Si (hydr)oxides, with Emphasis on Nanosized Gibbsite (α-Al(OH)$_3$), Umeå University, Sweden, 2002.
[18] Th. Fanghänel, J.I. Kim, R. Klenze, Y. Kato, J. Alloys Compd. 225 (2000) 308–311.
[19] T. Kimura, G.R. Choppin, Y. Kato, Z. Yoshida, Radiochim. Acta 72 (1996) 61–64.
[20] J.V. Beitz, D.L. Bowers, M.M. Doxtader, V.A. Maroni, D.T. Reed, Radiochim. Acta 44–45 (1988) 87–93.
[21] Th. Rabung, Th. Stumpf, H. Geckeis, R. Klenze, J.I. Kim, Radiochim. Acta 88 (2000) 711–716.
[22] N.M. Edelstein, R. Klenze, Th. Fanghänel, S. Hubert, Coord. Chem. Rev. 250 (2006) 948–973.
[23] R.M. Smith, A.E. Martell, Critically Selected Stability Constants of Metal Complexes, Version 6.0, National Institute of Standards and Technology, Gaithersburg, MD, 2001.
[24] H. Brandt, D. Bosbach, P.J. Panak, Th. Fanghänel, Geochim. Cosmochim. Acta 71 (2007) 145–154.
[25] Th. Stumpf, C. Hennig, A. Bauer, M.A. Denecke, Th. Fanghänel, Radiochim. Acta 92 (2004) 133–138.
[26] Z. Zhang, P. Fenter, L. Cheng, N.C. Sturchio, M.J. Bedzyk, M. Predot, A. Bandura, J.D. Kubicki, S.N. Lvov, P.T. Cummings, A.A. Chialvo, M.K. Ridley, P. Benezeth, L. Anovitz, D.A. Palmer, M.L. Machesky, D.J. Wesolowski, Langmuir 20 (2004) 4954–4969.
[27] Th. Stumpf, Th. Fanghänel, J. Colloid Interface Sci. 249 (2002) 119–122.